Struct Multidisc Optim 24, 51–59
Digital Object Identifier (DOI) 10.1007/s00158-002-0213-3

Efficient optimization of a noise transfer function by modification of a shell structure geometry – Part I: Theory*

S. Marburg

Abstract In the early stages of vehicle body development trends for the acoustic behaviour of the whole vehicle are, on the one hand, of great importance, but difficult to achieve. Geometry based, parametric model descriptions and optimization techniques enable the engineer to find out these trends. This paper starts with a review of structural acoustic sensitivity analysis and optimization. Then, the noise transfer function including structural harmonic analysis, acoustic influence coefficients and their coupling is described. This is followed by some remarks on the optimization process, discussing objective functions, useful design parameters and optimization techniques. Finally, a section on sensitivity analysis presents a numerical and a semianalytic method. In the case of small design modifications the sensitivity calculation mainly reduces to the well-known semianalytic calculation of harmonic displacement sensitivities. Part II presents the design optimization of a sedan dashboard.

Key words structural acoustics, noise transfer function, sound pressure level, acoustic influence coefficients, geometry optimization, semianalytic sensitivity analysis

1 Introduction

Acoustic behaviour inside the cabin is becoming more and more of a challenge for the car manufacturer. To find out trends in the early stages of body development seems to be an important task since during this period the design of the panels is created. Hardly any changes can be included once the body has been designed.

On this topic, related publications either provide fully coupled (structure fluid interaction model) noise transfer functions (e.g. Yashiro *et al.* 1985), or noise transfer functions based on the one way structure fluid coupling model described later (e.g. Suzuki 1989). In other related work, structural transfer functions are applied to quantify acoustic behaviour (e.g. Giebeler and Booz 1994).

There are a number of articles on general sensitivity calculation of structural and acoustic analysis. For sensitivity calculation in structural analysis we refer to a review paper by Haftka and Adelman (1989). An extensive numeric study was provided by Kibsgaard (1992). Structural optimization with respect to acoustic properties, i.e. the adaptation of natural frequencies to certain requirements is found in the review paper by Grandhi (1993). Hinton *et al.* (1995) applied shape optimization techniques to obtain optimal shell geometry and thickness distribution with the objective of a maximized fundamental frequency of structures. Modal sensitivity analysis of the fully coupled structural acoustic system has been accomplished by Ma and Hagiwara (1991a). Acoustic sensitivity analysis is reported by Bernhard (1985), Kane *et al.* (1991), Cunefare and Koopmann (1992) or Meric (1996). These papers mainly consider sensitivity analysis for the Helmholtz equation using special finite or boundary element formulations. In his dissertation, Hibinger (1998) described techniques for minimization of structure-borne noise levels. Moreover, he maximized eigenfrequencies and included mass restrictions while using plate and shell thicknesses and ribs as parameters. Experimental verification was provided for the example of two plates perpendicular to each other.

Structural and acoustic optimization of noise transfer functions has been carried out by many authors. However, there are some papers that indicate optimization methods whereby the optimization is carried out

Received February 2, 2001
Received by Design Optimization September 13, 1999

S. Marburg

Institut für Festkörpermechanik, Technische Universität, 01062 Dresden, Germany
e-mail: marburg@ifkm.mw.tu-dresden.de

* This paper was originally submitted to and accepted by the discontinued journal *Design Optimization*

using certain trial and error methods, also combined with suitable measurements for identification of sources (see, for example Eichlseder and Dannbauer 1994; Mühlmeier *et al.* 1994). Vehicle interior noise was decreased by application of a suitable sensitivity analysis in the papers by Hagiwara *et al.* (1991), Ma and Hagiwara (1991b). The fully coupled structural acoustic system was solved. They used the plate thicknesses as design parameters. Lamancusa (1993) and Belegundu *et al.* (1994) investigated and optimized rectangular plates and their radiation characteristics. Design parameters were stepped plate thicknesses and the radiated sound power was used as the objective function. Hambric (1995) and Hambric (1996) described optimization techniques and an optimization code that may be used to reduce noise. They calculated sensitivities by global finite differences. The design parameters mainly included shell thickness, material loss factors or stiffening ribs. Pal and Hagiwara (1994) provided a fully coupled structural acoustic noise transfer function optimization by modal sensitivity analysis. Furthermore, as the modal characteristics of the fluid domain did not change during the optimization process they had to calculate the fluid modes only once in a first step. Again, the design parameter was a plate thickness. Christensen *et al.* (1998) reviewed analysis and optimization techniques in structural acoustics. Another recent paper by Christensen and Olhoff (1998) presents an application to the finding of the shape of a loudspeaker diaphragm. As the objective function a desired directivity pattern is used whereas the shape of the axisymmetric diaphragm shell is defined by eight parameters forming a quadratic B-spline spanned by nine points. Marburg *et al.* (1997a) and Marburg *et al.* (1997b) illustrate the power of design optimization for real geometries for a vehicle roof.

In some cases, where the geometry of a shell was modified in an optimization process, unexpected high improvements of the noise radiation or the noise transfer functions were observed and described. This is mainly due to the great influence of the shell curvature on the shell stiffness.

This first part of the articles aims to present a methodology to calculate a noise transfer function and creates an objective function that may be used as a valuation criterion of a certain model. The discussion of fast optimization procedures is closely linked with the definition of parameters and an efficient sensitivity analysis. As this methodology deals with the modification of a model a realistic model is required. It is not the target of this paper to explain modelling and validation. These parts will be presupposed for this article although they obviously require most expenditure of manual and computational work.

Part II of this paper presents the application of the above methodology to the shell model of a vehicle dashboard. The choice of parameters and their constraints will be discussed as well as the objective function. Finally, the new design and vibrational behaviour is illustrated.

2 Noise transfer function

2.1 General considerations

In this article, the *noise transfer function* is calculated as the sound pressure level at a certain fluid field point due to a force excitation at the surrounding structure. This is illustrated for the special case of interior noise problems of a vehicle cabin in Fig. 1. It is mentioned that this consideration mainly focuses on interior problems since for exterior problems in structural acoustics it is more sensible to use the radiated sound power due to a force excitation as the noise transfer function (Christensen *et al.* 1998).

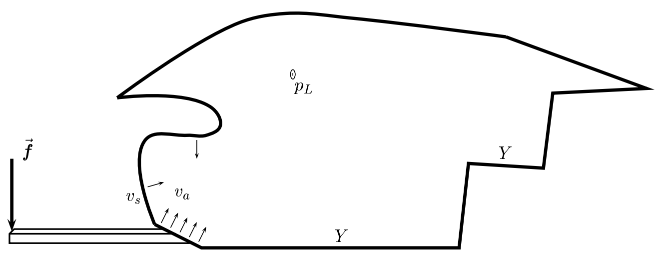

Fig. 1 Vehicle body and cabin compartment: Noise transfer function, i.e. sound pressure level p_L at the drivers ear due to force excitation $f(\mathbf{x}, \omega)$ (20) and (21)

The calculation procedure consists of three parts, the structural harmonic analysis, the acoustic harmonic analysis and the coupling of both. A one-way-model for the structure-fluid-interaction is applied. This model contains the fluid excitation by the structure but structural excitation by the fluid is not included. This type of structure-fluid-interaction is reasonable for vehicle body applications since the structure consists of certain heavy material – often steel – and the fluid – air – is light. For application of a light structure or/and a heavy fluid a structure-fluid-interaction in both directions should be preferred.

Most interesting for the following considerations is the time harmonic case. For this reason, we consider that all time-dependent functions $F(\mathbf{x}, t)$ are time-harmonic functions where the spatial variable $\mathbf{x}$ and the time variable t are separated as

$$F(\mathbf{x}, t) = f(\mathbf{x})\, e^{i\omega t}\,. \tag{1}$$

In this equation ω is the circular frequency and i the imaginary unit where $i^2 = -1$.

2.2 Structural analysis

Discretizing a shell structure into finite elements and introducing the above time dependency, the equations of motion yield the well-known system of linear complex equations of the harmonic analysis (cf. Bathe 1982)

$$\mathbf{A}(\omega)\mathbf{u}(\omega) = \mathbf{f}(\omega)\,, \tag{2}$$

where $\mathbf{u}$ and $\mathbf{f}$ describe the column matrices containing the nodal displacement vectors and the nodal excitation force vectors; $\mathbf{A}$ is the global system matrix of finite elements more commonly known as the dynamic stiffness matrix given by

$$\mathbf{A}(\omega) = \mathbf{K} + i\omega\mathbf{B} - \omega^2\mathbf{M}\,. \tag{3}$$

In (3) the matrices $\mathbf{K}$, $\mathbf{B}$ and $\mathbf{M}$ represent the (static) stiffness matrix, the damping matrix and the mass matrix.

A simple inversion of the dynamic stiffness matrix provides the nodal displacement vectors formally written as

$$\mathbf{u}(\omega) = \mathbf{A}^{-1}(\omega)\mathbf{f}(\omega)\,. \tag{4}$$

Time derivation of the nodal displacement vector $\mathbf{u}$ leads to the nodal velocity vector $\mathbf{v}$ as

$$\mathbf{v}(\omega) = i\,\omega\mathbf{u}(\omega)\,. \tag{5}$$

The nodal particle velocity of the shell structure v_s is defined as the normal component of the nodal velocity vector given by

$$v_s(\omega) = \mathbf{n}\cdot\mathbf{v}(\omega) = i\omega\mathbf{n}\cdot\mathbf{u}(\omega)\,. \tag{6}$$

Assembling the components of the nodal normal vectors $\mathbf{n}$ into a matrix $\mathbf{N}$, the column matrix of the structural particle velocity is written in terms of the nodal displacements by

$$\mathbf{v}_s(\omega) = i\omega\mathbf{N}\mathbf{u}(\omega)\,, \tag{7}$$

and in terms of the force excitation and the system properties as

$$\mathbf{v}_s(\omega) = i\omega\mathbf{N}\mathbf{A}^{-1}(\omega)\mathbf{f}(\omega)\,. \tag{8}$$

The nodal particle velocity is then used as a coefficient of the Robin boundary condition in acoustic analysis.

2.3 Acoustic analysis

The acoustic analysis is reduced to the calculation of discrete and continuous acoustic influence coefficients also known as sensitivities. These influence coefficients were first calculated by Ishiyama *et al.* (1988). A more detailed discussion of their determination and their application are given by Marburg (1996) and Marburg *et al.* (1997a). One possible method to determine discrete and continuous acoustic influence coefficients, $b(\omega)$ and $\beta(\omega)$ is briefly reviewed in the following.

To solve the boundary value problem for the harmonic wave equation – the Helmholtz equation – the surface of the considered fluid-filled cabin is discretized into boundary elements. Applying a boundary collocation method, a linear system of equations as

$$\mathbf{H}(\omega)\mathbf{p}(\omega) = \mathbf{G}(\omega)\mathbf{v}_f(\omega) \tag{9}$$

is found. The nodal values of the sound pressure p and these of the fluid's particle velocity v_f correspond to the Dirichlet and Neumann acoustic boundary data. The global system matrices $\mathbf{G}$ and $\mathbf{H}$ are well-known from boundary element analysis. The sound pressure p_i at a point inside the cabin – in this article mostly called the interior point or the driver's ear – is calculated in terms of column matrices $\mathbf{g}$ and $\mathbf{h}$ and their scalar multiplication with the boundary data $\mathbf{u}$ and $\mathbf{v}_f$. We find p_i as

$$p_i(\omega) = \mathbf{g}^T(\omega)\mathbf{v}_f(\omega) - \mathbf{h}^T(\omega)\mathbf{p}(\omega)\,. \tag{10}$$

In a further step one has to incorporate the Robin boundary condition, the so-called admittance formulation (cf. Suzuki 1989) into (9) and (10). It is locally given by

$$v_f(\omega) - v_s(\omega) = Y(\omega)p(\omega)\,. \tag{11}$$

The coefficient Y denotes the acoustic boundary admittance. The diagonal matrix $\mathbf{Y}$ contains the nodal values of the boundary admittance. Thus, (9) changes into

$$\left[\mathbf{H}(\omega) - \mathbf{G}(\omega)\mathbf{Y}(\omega)\right]\mathbf{p}(\omega) = \mathbf{G}(\omega)\mathbf{v}_s(\omega)\,, \tag{12}$$

and for (10) we obtain

$$p_i(\omega) = \mathbf{g}^T(\omega)\mathbf{v}_s(\omega) - \left[\mathbf{h}^T(\omega) - \mathbf{g}^T(\omega)\mathbf{Y}(\omega)\right]\mathbf{p}(\omega)\,. \tag{13}$$

Substitution of $\mathbf{p}$ in (13) by isolating $\mathbf{p}$ in (12) the sound pressure at the internal point is found to be (omitting ω-dependence)

$$p_i = \left\{\mathbf{g}^T - \left[\mathbf{h}^T - \mathbf{g}^T\mathbf{Y}\right]\left[\mathbf{H} - \mathbf{G}\mathbf{Y}\right]^{-1}\mathbf{G}\right\}\mathbf{v}_s\,, \tag{14}$$

which can be written in short form as

$$p_i(\omega) = \mathbf{b}^T(\omega)\mathbf{v}_s(\omega)\,. \tag{15}$$

The discrete influence coefficients b_k represent the solution of the acoustic boundary value problem for just one internal point excluding the particle velocity as a boundary condition. Furthermore, they account for the sound pressure sensitivity at the internal point with respect to a structural vibration at a certain mesh point. The nodal product of $b_k v_k$ provides the contribution of the mesh point k to the sound pressure at the internal point.

As these influence coefficients are discrete they are not suited for visualization or for mesh interpolation and transformation. For this reason, it is useful to transform them into continuous influence coefficients β on behalf of the relation

$$p_i(\omega) = \mathbf{b}^T(\omega)\mathbf{v}_s(\omega) = \int_\Gamma \beta(\omega) v_s(\omega)\,\mathrm{d}\Gamma\,, \tag{16}$$

where Γ represents the fluid's surface. Furthermore, the continuous data on the right-hand side of (16), β and v_s, are substituted by shape functions φ_j, i.e. piecewise formulated polynomials (Lagrangian polynomials), and nodal values. For the particle velocity, the column matrix $\mathbf{v}_s$ contains the same nodal values as on the left-hand side of (16). The nodal values of the continuous influence coefficients are assembled in $\boldsymbol{\beta}$. We can write

$$\mathbf{b}^T(\omega)\mathbf{v}_s(\omega) = \boldsymbol{\beta}^T(\omega) \int_\Gamma \boldsymbol{\Phi}^T \boldsymbol{\Phi}\,\mathrm{d}\Gamma\,\mathbf{v}_s(\omega)\,, \tag{17}$$

where the column matrix $\boldsymbol{\Phi}$ contains the shape functions φ_j. Introducing a sparse symmetric matrix $\boldsymbol{\Theta}$ as

$$\Theta_{ik} = \int_\Gamma \varphi_i(\mathbf{x})\varphi_k(\mathbf{x})\,\mathrm{d}\Gamma(\mathbf{x})\,, \tag{18}$$

we are able to transform discrete into continuous influence coefficients

$$\boldsymbol{\beta}(\omega) = \boldsymbol{\Theta}^{-1}\mathbf{b}(\omega)\,, \tag{19}$$

and continuous into discrete influence coefficients by

$$\mathbf{b}(\omega) = \boldsymbol{\Theta}\boldsymbol{\beta}(\omega)\,. \tag{20}$$

As mentioned above, the calculation of acoustic influence coefficients is independent from the solution of the structural boundary value problem.

2.4 Coupling of structure and fluid model

The separate solution of structural and acoustic analysis enables us to use different meshes for both. Since we mainly consider vehicle interior noise problems, we deal with the problem that the fluid mesh may be much coarser then the mesh of the shell structure of the body. Applying (16) to the coarse boundary element mesh of the fluid continuous influence coefficients can be determined. Extracting the continuous coefficients at the nodes of the more detailed mesh of the structure one can find the discrete coefficients by multiplying them by $\boldsymbol{\Theta}_s$ where $\boldsymbol{\Theta}_s$ is now assembled for the fine mesh. Applying these discrete influence coefficients to the detailed mesh of the structure we can express the sound pressure at the internal point due to a specified force excitation by substituting $\mathbf{v}_s$, (15) by (8). This yields

$$p_i(\omega) = i\omega\mathbf{b}^T(\omega)\mathbf{N}\mathbf{A}^{-1}(\omega)\mathbf{f}(\omega)\,. \tag{21}$$

In this equation, $\mathbf{b}$ is the column matrix of the discrete acoustic influence coefficients of the fine structural mesh. The main objective of our investigation is the decrease of the noise inside a cabin. The perceived loudness of sound (in the required frequency domain ≤ 200 Hz) is virtually proportional to the logarithmic sound pressure. For that, the transformation of the noise transfer function into a sound pressure level p_{L} is useful. This leads to

$$p_{\mathrm{L}}(\omega) = L\left\{p_i(\omega)\right\} = 20\log_{10}\left(\frac{|p_i(\omega)|}{p_0}\right)\,. \tag{22}$$

The reference sound pressure is given by $p_0 = 2\cdot 10^{-5}$ Pa. The unit of p_{L} is dB.

Herein, the sound pressure level at the internal point due to a force excitation, (22) with the substitution of p_i from (21), is called the *noise transfer function*. An illustration is given by Fig. 1 for the special case of a vehicle cabin compartment.

3 Optimization process

3.1 Objective function

As the sound pressure level still depends on the frequency an integral criterion over the whole frequency domain is required. A solution that meets both mathematical and technical interests is the following averaging

$$F = \frac{1}{\omega_{\max} - \omega_{\min}} \int_{\omega_{\min}}^{\omega_{\max}} \Phi\left\{p_{\mathrm{L}}(\omega)\right\}\,\mathrm{d}\omega\,. \tag{23}$$

The operator $\Phi\{\}$ applied to p_{L} represents a kind of a weighting function. An example for this weighting function is

$$\Phi\left\{p_{\mathrm{L}}\right\} = \begin{cases} \left(p_{\mathrm{L}} - p_{\mathrm{Ref}}\right)^n & \text{for} \quad p_{\mathrm{L}} > p_{\mathrm{Ref}} \\ 0 & \text{for} \quad p_{\mathrm{L}} \leq p_{\mathrm{Ref}}\,. \end{cases} \tag{24}$$

The exponent n controls the type of average. For $n = 1$ (24) leads to the mean value where only values higher than a certain reference level p_{Ref} are taken into account. Similarly, for $n = 2$ this form provides the squared mean value.

The major advantage of the $n = 2$ form is that high level peaks are higher valued than low level parts of the function. This helps to reduce these high level peaks during an optimization procedure and avoids deep valleys as compensation of high peaks.

The choice of the reference level p_{Ref} meets technical requirements as values below are not considered. So they cannot be overvalued. On the other hand, a reference level higher than the sound pressure level minimum destroys the C^1 continuity of function F in (23).

3.2 Design parameters

A parametric description of the geometry requires the introduction of design parameters. The parameters used here are assembled into the vector $\boldsymbol{\vartheta}$. Moreover, all parameters describe the position of single *keypoints*, which is a similar definition to that in the paper by Christensen and Olhoff (1998) and the same that was used by Marburg *et al.* (1997a) and Marburg *et al.* (1997b). A whole set of *keypoints* – only some of them have parametric coordinates – defines the complete geometry of a shell structure since they are connected by (interpolated) *lines* and *areas* are interpolated between the *lines*. Meshing of *areas* provides the finite element mesh that consists of *nodes* and *elements*. An illustration of the effect of a parameter modification is given in Fig. 2. The sketch shows the position vectors of certain *keypoints* P_1 and P_3. Modification of design parameter ϑ_3 only effects the position of P_3. The connecting *line* is interpolated by cubic splines. Consequently, this *line* is modified as well as the interpolated *areas* not shown in this figure.

Highly efficient sensitivity analysis and thus, a fast optimization process require some presumptions concerning the parameters. These are the following.

(a) It is presumed that all the modification of the geometry of the shell structure are small with respect to the fluid's wave length.
(b) It is presumed that all the modification of the geometry of the shell structure are small with respect to the shell structure size.
(c) It is presumed that the modification mainly shifts the surface shell in its normal direction.
(d) It is presumed that the modification does not effect the force excitation of the structure.

All these presuppositions and their conclusions simplify the sensitivity analysis and the optimization process.

Assumption (a) leads to the conclusion that the discrete acoustic influence coefficients do not depend on the parameter set

$$\frac{\partial \mathbf{b}}{\partial \boldsymbol{\vartheta}} = \mathbf{0} \,. \tag{25}$$

That means, that the discrete influence coefficients are calculated only once. They can be used for each optimization step. However, this requires a constant topology of the mesh of the structure during the whole optimization process. If this cannot be ensured one can start with the continuous influence coefficients of the coarser fluid mesh and extract them at the new fine mesh. The new discrete influence coefficients are then determined by (20).

Consequence of the assumptions (b) and (c) is that the normal vectors do not depend on the parameter set

$$\frac{\partial \mathbf{N}}{\partial \boldsymbol{\vartheta}} = \mathbf{0} \,, \tag{26}$$

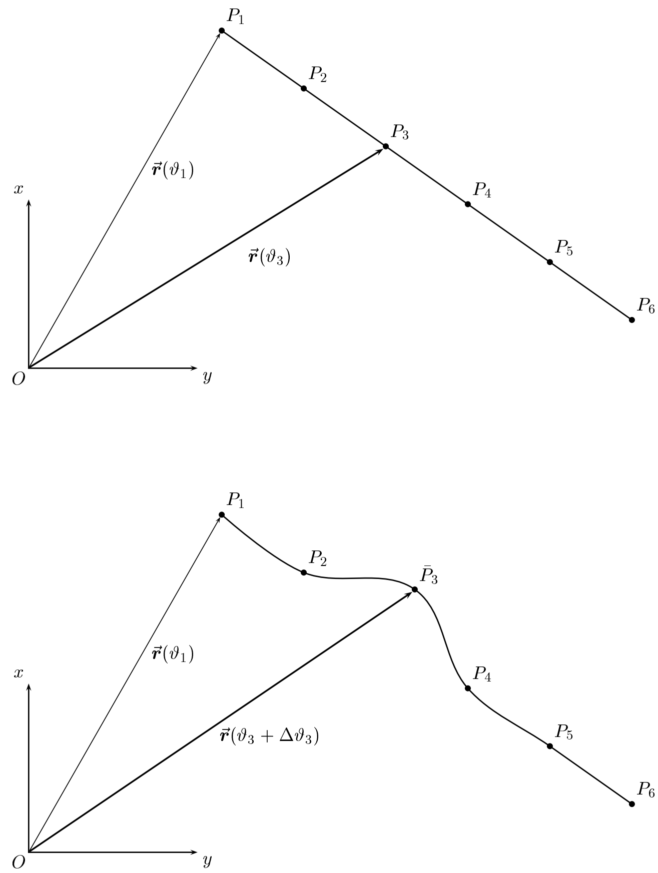

Fig. 2 Illustration of parametrically defined *keypoint* positions and effect of single parameter modification to *line* curvature

whereas the assumption (d) formulates the excitation force independence of the parameters as

$$\frac{\partial \mathbf{f}}{\partial \boldsymbol{\vartheta}} = \mathbf{0} \,. \tag{27}$$

Hence, the objective function F in terms of the parameter set $\boldsymbol{\vartheta}$ can be written as

$$F(\boldsymbol{\vartheta}) = \frac{1}{\omega_{\max} - \omega_{\min}} \int\limits_{\omega_{\min}}^{\omega_{\max}} \Phi \left\{ p_{\mathrm{L}}(\omega, \boldsymbol{\vartheta}) \right\} \, \mathrm{d}\omega \,, \tag{28}$$

with the substitution

$$p_{\mathrm{L}}(\omega) = 20 \log_{10} \left(\frac{\left| i\omega \mathbf{b}^T(\omega) \mathbf{N} \mathbf{A}^{-1}(\omega, \boldsymbol{\vartheta}) \mathbf{f}(\omega) \right|}{p_0} \right) \,. \tag{29}$$

As the reader should now be familiar with the dependencies on ω it will not be explicitly mentioned in the following sections.

3.3 Optimization strategy

There is no optimum optimization strategy for every optimization problem. So one has to look for an appropriate one. As this article deals with rather complex and nonlinear dependencies between parameters and objective functions a technique that combines both stochastic and deterministic algorithms is required. One possibility is to use both a random iteration and the know-how of the engineers for finding suitable initial parameter vectors. In the publications on structural acoustic optimization mostly gradient based techniques were reported to decrease noise transfer functions or radiated noise (Christensen and Olhoff 1998; Hambric 1995; Pal and Hagiwara 1994).

The objective function covers a whole frequency domain. Within this domain the number of vibration modes can easily reach 200 and more. For that reason and because of rather complicated shell geometries it is difficult to estimate an useful initial parameter set. Thus random iterations and reasonable trials should complement each other.

The crucial part in optimization is the first order or gradient method. This method requires sensitivities for calculation of the gradient which is the subject of the following section. This gradient approximation is followed by a line search algorithm in order to provide a new reference value. Most important in the first-order method is the step size for the numeric sensitivity analysis and for the line search algorithm. The step size in the sensitivity analysis must be at least of such a size that the sensitivities are not overly influenced by round off errors and it must be small enough that linearization around a reference point is still acceptable. The interval may be really small or (in some cases) may not exist. The latter case would require special treatment of the parameter. One possibility is to exclude this parameter from the optimization process at least for some loops.

Finally, concerning optimization must be mentioned that for most technical applications it is not necessary to find the optimum. Mainly, one looks for significant improvements of the *noise transfer function* resulting in a decrease of the objective function (28). The actual search for the optimum is probably most inefficient for technical problems where as many as 10 to 50 or even more parameters have to be optimized.

4 Sensitivity analysis

4.1 Finite differences numerically determined

The most simple way of calculating sensitivities is the numerical determination of finite differences. The sensitivity of the objective function F with respect to a single parameter ϑ_k can be written by

$$\frac{\partial F(\vartheta_k)}{\partial \vartheta_k} = \frac{F(\vartheta_k + \Delta\vartheta_k) - F(\vartheta_k)}{\Delta\vartheta_k} + O\left(\Delta\vartheta_k \frac{\partial^2 F}{\partial \vartheta_k^2}\right) . \tag{30}$$

Reducing this approximation to the difference quotient (30) changes into

$$\frac{\partial F(\vartheta_k)}{\partial \vartheta_k} \approx \frac{\Delta F(\vartheta_k)}{\Delta\vartheta_k} = \frac{F(\vartheta_k + \Delta\vartheta_k) - F(\vartheta_k)}{\Delta\vartheta_k} . \tag{31}$$

As the objective function $F(\boldsymbol{\vartheta})$ is a strongly nonlinear function calculation of sensitivities using (31) may possibly lead to cumbersome and unexpected results. These effects may be consequences of unsuitably chosen step sizes $\Delta\vartheta_k$. However, they can hardly be avoided in the case of a strongly nonlinear objective function. Nevertheless, the risk of cumbersome results in sensitivity analysis via global finite differences may be decreased by an improved step size control or by using a three point approximation. Then, the derivative is

$$\frac{\partial F(\vartheta_k)}{\partial \vartheta_k} = \frac{F(\vartheta_k + \Delta\vartheta_k) - F(\vartheta_k - \Delta\vartheta_k)}{2\Delta\vartheta_k} + O\left[(\Delta\vartheta_k)^2 \frac{\partial^3 F}{\partial \vartheta_k^3}\right] . \tag{32}$$

Although (32) requires only two calculations of F, the value of $F(\vartheta_k)$ is still required as a reference value for the line search algorithm in optimization.

This type of approximation of differentiation can be very easily applied to commercial computer codes since the sensitivity calculation may be independently carried out only by modifying a single parameter. Although mathematically not correct one can easily calculate sensitivities for C^0 continuous objective functions.

However, this implies that for m parameters the *noise transfer function*, (21), has to be calculated $m+1$ times for a sensitivity analysis applying (30) and $2m+1$ times when using (32). Even with all the simplifications, (25) to (27), one has to carry out the structural analysis, (4). For large scale problems, e.g. geometry optimization of a whole vehicle body, it is necessary to find much more efficient procedures for sensitivity analysis. One of these will be described in the following.

4.2 More efficient semianalytic sensitivity analysis

A more efficient method of sensitivity analysis is known as the *semianalytic method* (see for example Haftka and Adelman 1989; Kibsgaard 1992). For that, the calculation of sensitivities of the structural displacements is based on implicit differentiation of the linear system of equations (2). The derivative of (2) with respect to one design parameter ϑ_k is given by

$$\frac{\partial \mathbf{A}}{\partial \vartheta_k}\mathbf{u} + \mathbf{A}\frac{\partial \mathbf{u}}{\partial \vartheta_k} = \frac{\partial \mathbf{f}}{\partial \vartheta_k} . \tag{33}$$

Recalling the assumption that the excitation force vector does not depend on the parameters, (27) and rearrangement of (33) produce a linear system of equations

$$\mathbf{A}\frac{\partial \mathbf{u}}{\partial \vartheta_k} = -\frac{\partial \mathbf{A}}{\partial \vartheta_k}\mathbf{u}\,, \tag{34}$$

that has the same system matrix as (2). The only difference is the load vector on the right hand side. However, if (2) is solved by modal superposition one can use the same modes for the solution of (34). Because this method is really a numeric method which applies some algebraic transformations in a reasonable way, it was called *semi-analytic*. Formally, the sensitivities of the structural displacements can be written as

$$\frac{\partial \mathbf{u}}{\partial \vartheta_k} = -\mathbf{A}^{-1}\frac{\partial \mathbf{A}}{\partial \vartheta_k}\mathbf{u}\,. \tag{35}$$

Splitting matrix $\mathbf{A}$ into its components, (3), yields

$$\frac{\partial \mathbf{A}}{\partial \vartheta_k} = \frac{\partial \mathbf{K}}{\partial \vartheta_k} + i\omega\frac{\partial \mathbf{B}}{\partial \vartheta_k} - \omega^2\frac{\partial \mathbf{M}}{\partial \vartheta_k}\,. \tag{36}$$

As we assume a parameter independent modal damping the term including $\mathbf{B}$ in (36) vanishes. Obviously, it follows from the presumptions made in the previous section that the sensitivity of the mass matrix is much smaller than that of the stiffness matrix as the curvature geometry essentially controls the shell stiffness where a small modification of the curvature hardly effects mass and inertia properties. However, the mass matrix derivative is multiplied by ω^2. For a frequency of 200 Hz this factor is greater than 10^6! So even small modifications in the mass matrix may significantly influence the sensitivity of the dynamic stiffness matrix. Simplified, we formulate

$$\frac{\partial \mathbf{A}}{\partial \vartheta_k} = \frac{\partial \mathbf{K}}{\partial \vartheta_k} - \omega^2\frac{\partial \mathbf{M}}{\partial \vartheta_k}\,. \tag{37}$$

Note, that the sensitivity of A is real since the damping matrix is excluded.

Analytic differentiation of the objective function F reduces to the differentiation of function Φ with respect to ϑ_k as

$$\frac{\partial F(\vartheta_k)}{\partial \vartheta_k} = \frac{1}{\omega_{\max}-\omega_{\min}}\int\limits_{\omega_{\min}}^{\omega_{\max}}\frac{\partial \Phi\left\{p_{\mathrm{L}}(\vartheta_k)\right\}}{\partial \vartheta_k}\,\mathrm{d}\omega\,. \tag{38}$$

Since analytic differentiation of Φ requires a C^1 continuity the bottom line in (24) is skipped for the following considerations. So Φ is reduced to

$$\Phi\left\{p_{\mathrm{L}}(\vartheta_k)\right\} = \left[p_{\mathrm{L}}(\vartheta_k) - p_{\mathrm{Ref}}\right]^n\,, \tag{39}$$

and its derivative yields

$$\frac{\partial \Phi\left\{p_{\mathrm{L}}(\vartheta_k)\right\}}{\partial \vartheta_k} = n\left[p_{\mathrm{L}}(\vartheta_k) - p_{\mathrm{Ref}}\right]^{n-1}\frac{\partial p_{\mathrm{L}}(\vartheta_k)}{\partial \vartheta_k}\,. \tag{40}$$

Thus, the sensitivity analysis of the objective function requires differentiation of the sound pressure level.

Returning to (29) and introducing the substitutions (skipping ϑ_k-dependencies)

$$c_1 = \frac{10}{\ln 10}\,,\quad c_2 = \frac{i\omega}{p_0}\,,$$

and

$$\tilde{p}_i = \mathbf{b}^T\mathbf{N}\mathbf{A}^{-1}\mathbf{f} = \mathbf{b}^T\mathbf{N}\mathbf{u}\,, \tag{41}$$

an equivalent form of that equation is found to be

$$p_{\mathrm{L}} = \frac{c_1}{2}\ln\left[c_2\left|\tilde{p}_i(\vartheta_k)\right|\right]\,. \tag{42}$$

Further, this is equivalent to

$$p_{\mathrm{L}} = c_1\ln\left[c_2\left|\tilde{p}_i(\vartheta_k)\right|^2\right] =$$

$$c_1\ln\left\{c_2\left[\mathcal{R}^2\left\langle\tilde{p}_i(\vartheta_k)\right\rangle + \mathcal{I}^2\left\langle\tilde{p}_i(\vartheta_k)\right\rangle\right]\right\}\,, \tag{43}$$

where $\mathcal{R}\langle\tilde{p}_i\rangle$ and $\mathcal{I}\langle\tilde{p}_i\rangle$ represent real and imaginary parts of $\tilde{p}_i$, respectively. After differentiating (43) with respect to ϑ_k the constant c_2 vanishes. We find

$$\frac{\partial p_{\mathrm{L}}}{\partial \vartheta_k} =$$

$$2c_1\frac{\mathcal{R}\left\langle\tilde{p}_i(\vartheta_k)\right\rangle\dfrac{\partial \mathcal{R}\left\langle\tilde{p}_i(\vartheta_k)\right\rangle}{\partial \vartheta_k} + \mathcal{I}\left\langle\tilde{p}_i(\vartheta_k)\right\rangle\dfrac{\partial \mathcal{I}\left\langle\tilde{p}_i(\vartheta_k)\right\rangle}{\partial \vartheta_k}}{\mathcal{R}^2\left\langle\tilde{p}_i(\vartheta_k)\right\rangle + \mathcal{I}^2\left\langle\tilde{p}_i(\vartheta_k)\right\rangle} \tag{44}$$

Because ϑ_k is a real parameter the identities of

$$\frac{\partial \mathcal{R}\left\langle\tilde{p}_i(\vartheta_k)\right\rangle}{\partial \vartheta_k} = \mathcal{R}\left\langle\frac{\partial \tilde{p}_i(\vartheta_k)}{\partial \vartheta_k}\right\rangle$$

and

$$\frac{\partial \mathcal{I}\left\langle\tilde{p}_i(\vartheta_k)\right\rangle}{\partial \vartheta_k} = \mathcal{I}\left\langle\frac{\partial \tilde{p}_i(\vartheta_k)}{\partial \vartheta_k}\right\rangle \tag{45}$$

hold. The differentiation of $\tilde{p}_i$ with respect to ϑ_k can be written as

$$\frac{\partial \tilde{p}_i(\vartheta_k)}{\partial \vartheta_k} = \mathbf{b}^T\mathbf{N}\frac{\partial \mathbf{u}(\vartheta_k)}{\partial \vartheta_k}\,, \tag{46}$$

where the sensitivity of $\mathbf{u}$ is given in (35).

Summarizing the semianalytic sensitivity analysis, the sensitivity vector is calculated by the following equation and its substitutions (skipping dependencies)

$$\frac{\partial F}{\partial \boldsymbol{\vartheta}} = \frac{1}{\omega_{\max}-\omega_{\min}}\int\limits_{\omega_{\min}}^{\omega_{\max}}\left\{n\left[p_{\mathrm{L}} - p_{\mathrm{Ref}}\right]^{n-1}\frac{\partial p_{\mathrm{L}}}{\partial \boldsymbol{\vartheta}}\right\}\mathrm{d}\omega\,, \tag{47}$$

$$\frac{\partial p_{\mathrm{L}}}{\partial \boldsymbol{\vartheta}} = \frac{20}{\ln 10}\frac{\mathcal{R}\left\langle\tilde{p}_i\right\rangle\mathcal{R}\left\langle\tilde{p'}_i\right\rangle + \mathcal{I}\left\langle\tilde{p}_i\right\rangle\mathcal{I}\left\langle\tilde{p'}_i\right\rangle}{\mathcal{R}^2\left\langle\tilde{p}_i\right\rangle + \mathcal{I}^2\left\langle\tilde{p}_i\right\rangle}\,, \tag{48}$$

$$\tilde{p}_i = \mathbf{b}^T \mathbf{N} \mathbf{u}\,, \tag{49}$$

$$\tilde{p'}_i = \frac{\partial \tilde{p}_i}{\partial \vartheta_k} = \mathbf{b}^T \mathbf{N} \frac{\partial \mathbf{u}}{\partial \vartheta_k}\,, \tag{50}$$

and

$$\frac{\partial \mathbf{u}}{\partial \boldsymbol{\vartheta}} = -\mathbf{A}^{-1} \left[\frac{\partial \mathbf{K}}{\partial \boldsymbol{\vartheta}} - \omega^2 \frac{\partial \mathbf{M}}{\partial \boldsymbol{\vartheta}} \right] \mathbf{u}\,. \tag{51}$$

The derivatives of matrices $\mathbf{K}$ and $\mathbf{M}$ with respect to a single parameter ϑ_k are approximated either similar to sensitivity of F in (31)

$$\frac{\partial \mathbf{K}}{\partial \vartheta_k} \approx \frac{\mathbf{K}(\vartheta_k + \Delta\vartheta_k) - \mathbf{K}(\vartheta_k)}{\Delta\vartheta_k}\,,$$

and

$$\frac{\partial \mathbf{M}}{\partial \vartheta_k} \approx \frac{\mathbf{M}(\vartheta_k + \Delta\vartheta_k) - \mathbf{M}(\vartheta_k)}{\Delta\vartheta_k}\,, \tag{52}$$

or based on the type of equation (32) and skipping the error term

$$\frac{\partial \mathbf{K}}{\partial \vartheta_k} \approx \frac{\mathbf{K}(\vartheta_k + \Delta\vartheta_k) - \mathbf{K}(\vartheta_k - \Delta\vartheta_k)}{2\Delta\vartheta_k}\,,$$

and

$$\frac{\partial \mathbf{M}}{\partial \vartheta_k} \approx \frac{\mathbf{M}(\vartheta_k + \Delta\vartheta_k) - \mathbf{M}(\vartheta_k - \Delta\vartheta_k)}{2\Delta\vartheta_k}\,. \tag{53}$$

The step size for each parameter ϑ_k in the set $\boldsymbol{\vartheta}$ may be different.

In the set of equations (47)–(53), (49) probably appears computationally most costly. Although (48) looks complicated it is a simple combination of scalar complex values.

5 Summary

A review of structural acoustic optimization concepts in the Introduction was followed by the formulation of a noise transfer function. This function describes the sound pressure level at a certain field point due to a force excitation of the structure. The use of acoustic influence coefficients as the solution of the acoustic boundary value problem and the assumption of rather small design modifications simplify the optimization process and the sensitivity analysis. Thus, the well-known semianalytic method was adapted to sensitivity analysis of the sound pressure level at certain fluid field points.

The second part of this paper describes the design optimization of a sedan dashboard. Parameter studies and different choices of objective functions are discussed as well as the optimization strategy from an engineering point of view.

References

Bathe, K.-J. 1982: *Finite element procedures in engineering analysis*. Englewood Cliffs: Prentice Hall

Belegundu, A.D.; Salagame, R.R.; Koopmann, G.H. 1994: A general optimization strategy for sound power minimization. *Struct. Optim.* **8**, 113–119

Bernhard, R.J. 1985: A finite element method for synthesis of acoustical shapes. *J. Sound Vib.* **98**, 55–65

Christensen, S.T.; Olhoff, N. 1998: Shape optimization of a loudspeaker diaphragm with respect to sound directivity properties. *Control Cybernetics* **27**, 177–198

Christensen, S.T.; Sorokin, S.V.; Olhoff, N. 1998: On analysis and optimization in structural acoustics. Part I: problem formulation and solution techniques. *Struct. Optim.* **16**, 83–95

Cunefare, K.A.; Koopmann, G.H. 1992: Acoustic design sensitivities for structural radiators. *J. Vib. Acous.* **114**, 178–186

Eichlseder, W.; Dannbauer, H. 1994: Untersuchungen des akustischen Verhaltens einer Traktorkabine mit der Finite Elemente Methode. *XXIII Int. FEM Cong.* (held in Baden-Baden)

Giebeler, W.-R.; Booz, G. 1994: Akustisches Verhalten als Zielvorgabe in der Karosserieentwicklung. *Berechnung und Simulation im Fahrzeugbau*, pp. 237–252. VDI–Report 1153

Grandhi, R.V. 1993: Structural optimization with frequency constraints. *AIAA J.* **31**, 2296–2303

Haftka, R.T.; Adelman, H.M. 1989: Recent developments in structural sensitivity analysis. *Struct. Optim.* **1**, 137–151

Hagiwara, I.; Ma, Z.-D.; Arai, A.; Nagabuchi, K. 1991: Reduction of vehicle interior noise using structural-acoustic sensitivity analysis methods. *SAE Technical Paper Series No. 910208*

Hambric, S.A. 1995: Approximation techniques for broad–band acoustic radiated noise design optimization problems. *J. Vib. Acous.* **117**, 136–144

Hambric, S.A. 1996: Sensitivity calculations for broad–band acoustic radiated noise design optimization problems. *J. Vib. Acous.* **118**, 529–532

Hibinger, F. 1998: *Numerische Strukturoptimierung in der Maschinenakustik*. Dissertation, Technische Universität Darmstadt

Hinton, E.; Özakca, M.; Rao, V.R. 1995: Free vibration analysis and shape optimization of variable thickness plates, prismatic folded plates and curved shells. Part II: shape optimization. *J. Sound Vib.* **181**, 567–581

Ishiyama, S.-I.; Imai, M.; Maruyama, S.-I.; Ido, H.; Sugiura, N.; Suzuki, S. 1988: The application of ACOUST/BOOM – A noise level prediction and reduction code. *SAE–paper 880910*, pp. 195–205

Kane, J.H.; Mao, S.; Everstine, G.C. 1991: A boundary element formulation for acoustic shape sensitivity analysis. *J. Acous. Soc. Amer.* **90**, 561–573

Kibsgaard, S. 1992: Sensitivity analysis – the basis for optimization. *Int. J. Numer. Meth. Engrg.* **34**, 901–932

Lamancusa, J.S. 1993: Numerical optimization techniques for structural-acoustic design of rectangular panels. *Comp. & Struct.* **48**, 661–675

Ma, Z.-D.; Hagiwara, I. 1991a: Sensitivity analysis methods for coupled acoustic-structural systems. Part I: modal sensitivities. *AIAA J.* **29**, 1787–1795

Ma, Z.-D.; Hagiwara, I. 1991b: Sensitivity analysis methods for coupled acoustic–structural systems. Part II: direct frequency response and its sensitivities. *AIAA J.* **29**, 1796–1801

Marburg, S. 1996: Calculation and visualization of acoustic influence co-efficients in vehicle cabins using mode superposition techniques. In: Brebbia, C.A.; Martins, J.B.; Alibadi, M.H.; Haie, N. (eds.) *Boundary Elements XVIII* (Proc. 18th Int. Conf. on BEM, held in Braga, Portugal), pp. 13–22. Computational Mechanics Publications: Southampton

Marburg, S.; Hardtke, H.-J.; Schmidt, R.; Pawandenat, D. 1997a: An application of the concept of acoustic influence coefficients for the optimization of a vehicle roof. *Eng. Anal. Boundary Elements* **20**, 305–310

Marburg, S.; Hardtke, H.-J.; Schmidt, R.; Pawandenat, D. 1997b: Design optimization of a vehicle panel with respect to cabin noise problems. *Proc. NAFEMS World-Congr.*, pp. 885–896. Stuttgart

Meric, R.A. 1996: Shape design sensitivities and optimization for the nonhomogeneous Helmholtz equation by BEM. *Comm. Numer. Meth. Engrg.* **12**, 95–105

Mühlmeier, M.; Kumbein, T.; Vogler, N. 1994: Identifikation und Reduzierung der Flächenbeteiligungen am niederfrequenten Innenraumgeräusch. *Berechnung und Simulation im Fahrzeugbau*, pp. 221–235. VDI–Report 1153

Pal, C.; Hagiwara, I. 1994: Optimization of noise level reduction by truncated modal coupled structural-acoustic sensitivity analysis. *JSME Int. J., Series C* **37**, 246–251

Suzuki, S. 1989: Boundary element analysis of structural-acoustic problems with complicated boundary conditions. In: Brebbia, C.A.; Connor, J. (eds.) *Advances in boundary elements*, Vol. 2, pp. 341–353. Berlin, Heidelberg, New York: Springer

Yashiro, H.; Suzuki, K.; Kajio, Y.; Hagiwara, I.; Arai, A. 1985: An application of structural-acoustic analysis to car body structures. *Proc. SAE Surface Vehicle Noise and Vibration Conf.* (held in Traverse City, MI)